Int. J. Anal. Appl. (2026), 24:257

International Journal of Analysis and Applications

Global Stability of Two-Patch Within-Host HBV Infection Dynamics with Unidirectional Viral Spread

Raghad S. Alsulami[1,*], N. H. AlShamrani[2], A. M. Elaiw[1] and A. D. Hobiny[1]

[1]*Department of Mathematics, Faculty of Science, King Abdulaziz University, P.O. Box 80203, Jeddah 21589, Saudi Arabia*

[2]*Department of Mathematics and Statistics, College of Science, University of Jeddah, P.O. Box 80327, Jeddah 21589, Saudi Arabia*

[*]*Corresponding author:* ralsulami0525@stu.kau.edu.sa

Abstract. Hepatitis B virus (HBV) infects liver cells (hepatocytes). Persistent HBV infection may lead to the development of abnormal nodular formations within liver tissue. In this study, we propose and analyze a mathematical model describing the dynamics of a two-patch within-host HBV infection with unidirectional viral transmission from patch-1 to patch-2. The model captures interactions among six compartments: uninfected hepatocytes, infected hepatocytes, and free HBV particles in each of the two patches. A comprehensive mathematical analysis is carried out, including proofs of non-negativity and boundedness of solutions. The basic reproduction numbers in patch-1 (R_1) and patch-2 (R_2) are calculated using the next generation method. The global stability of all equilibrium points is rigorously examined using Lyapunov functions and LaSalle's invariance principle. Numerical simulations are conducted, demonstrating strong agreement with the analytical findings. Finally, sensitivity analysis identifies the key parameters influencing viral persistence.

1. Introduction

Reports from the World Health Organization (WHO) indicate that viral hepatitis leads to roughly 3,500 deaths each day, and this number continues to grow [1]. Globally, it is the second leading cause of death among infectious diseases, responsible for approximately 1.3 million deaths annually, a burden similar to that of tuberculosis [1].

Hepatitis B virus (HBV) is a DNA virus classified within the *Hepadnaviridae* family and replicates in the nuclei of liver cells [2]- [4]. Transmission pathways include mother-to-child transfer at birth, sexual contact, and exposure to contaminated blood or body fluids [5]. The likelihood of chronic

Received: Jun. 22, 2026.

2020 *Mathematics Subject Classification.* 34D20; 34D23; 37N25; 92B05.

Key words and phrases. Hepatitis B virus; two-patch; global stability; Lyapunov function; LaSalle's invariance principle.

https://doi.org/10.28924/2291-8639-24-2026-257
ISSN: 2291-8639

infection is strongly influenced by age: most adults successfully eliminate the virus, whereas infants and young children face a much higher risk of persistent infection [6], [7]. Persistent HBV infection over time may lead to severe liver injury, such as cirrhosis and hepatocellular carcinoma. Although antiviral therapies are available, complete viral clearance is rarely achieved [8], [9], underscoring the importance of integrating experimental findings with mathematical modeling to better capture disease dynamics.

To describe the progression of HBV infection from acute to chronic stages, researchers commonly rely on within-host mathematical models [10], which are adapted to reflect the specific biological features of the virus. Nowak et al. [11] introduced a basic viral dynamics model that has been widely adapted for HBV and other viral systems. In addition, a model incorporating the adaptive immune response in HBV infection was developed by Yousfi et al. [12].

Over time, several extensions and refinements of HBV models have been proposed. Manna et al. [13] introduced a model that accounts for HBV DNA-containing capsids, which was subsequently expanded by Manna [14] to incorporate CTL immune responses. Harroudi et al. [15] further improved this model by including antibody dynamics. Moreover, Xu et al. [16] examined a diffusive HBV model with time delay and a saturated infection rate. Geng et al. [17] studied HBV dynamics using a discrete-time framework with delays, while Elaiw et al. [18] explored a diffusive HBV model with generalized infection rates and CTL-mediated immunity. However, relatively limited attention has been given to modeling structural changes in liver tissue during disease progression, especially the transition from healthy tissue to fibrotic and cirrhotic states.

Four principal factors contribute to the pathogenesis of fibrotic and cirrhotic conditions, with the initial factor identified as recurrent episodes of inflammation, the subsequent factor being the apoptosis of hepatocytes, the third factor concerning the regenerative capacity of hepatocytes, and the final factor being the accumulation of fibrous tissue [19], [20]. All these factors lead to activation of collagen-producing cells, culminating in excessive accumulation of the extracellular matrix, the formation of pathological nodular structures (as shown in Figure 1), impaired liver function, and often the need for liver transplantation [21].

In chronic HBV infection, the loss of liver cells stimulates compensatory proliferation in the remaining hepatocytes. Meanwhile, the development of fibrosis and cirrhosis alters the physical and biological environment of the liver; increased tissue stiffness can exacerbate disease progression and may also affect viral replication behavior [23].

Several modeling studies suggest that spatial heterogeneity in hepatocyte turnover and liver structure may play a significant role in the persistence of HBV infection [24], [25]. In particular, differences in cell death and regeneration across fibrotic and cirrhotic regions have been considered. To capture these effects, two-region (two-patch) models incorporating heterogeneous viral replication have been proposed [21]. Such models investigate how variations in hepatocyte susceptibility and viral transport between distinct liver regions influence long-term infection outcomes. These

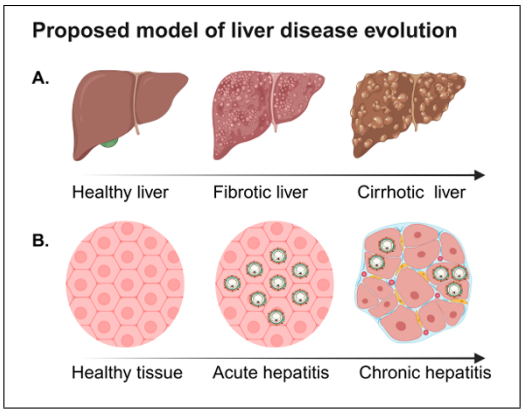

FIGURE 1. Schematic representation of liver disease progression following HBV infection: (A) the transition of the liver from a healthy state to fibrosis and eventually cirrhosis; (B) the distribution of HBV during the acute and chronic phases of infection. Figure created in [22]

findings highlight the importance of spatial structure within the liver in determining whether the virus is cleared or persists [21].

In the study [21], the authors analyze the equilibrium points and local stability of the system; however, fundamental qualitative properties, as well as global stability, are not addressed. Global asymptotic stability (GAS) is a stronger and more comprehensive notion of stability, in which the system trajectories converge to an equilibrium point from any admissible initial condition. This implies that any perturbations from equilibrium decay over time, ensuring that the system ultimately returns to its steady state regardless of the magnitude of the initial disturbance.

The two-patch within-host HBV infection model presented in [21] assumed that the host population is divided into two different patches, where each patch contains uninfected hepatocytes ($T_i(t)$), infected hepatocytes ($I_i(t)$), and free HBV particles ($V_i(t)$), for $i = 1, 2$. The model was formulated as:

$$
\begin{aligned}
\dot{T}_1 &= \overbrace{s_1}^{\substack{\text{Hepatocyte production rate in patch 1}\\ \text{Infectivity rate}}} - \overbrace{dT_1}^{\substack{\text{Uninfected hepatocyte death rate}\\ \text{Infected hepatocyte death rate}}} - \overbrace{\beta T_1 V_1}^{\text{Infectivity rate}}, \\
\dot{I}_1 &= \overbrace{\beta T_1 V_1}^{\text{Virus production rate}} - \overbrace{\delta I_1}^{\text{Virus clearance rate}}, \\
\dot{V}_1 &= \overbrace{\rho I_1}^{\substack{\text{Viral movement rate from patch 1 to patch 2}\\ \text{Hepatocyte production rate in patch 2}}} - \overbrace{cV_1}^{\text{Virus clearance rate}} - \overbrace{\phi V_1}^{\substack{\text{Uninfected hepatocyte death rate}\\ \text{Infectivity rate}}}, \\
\dot{T}_2 &= \overbrace{s_2}^{\substack{\text{Infectivity rate}\\ \text{Infected hepatocyte death rate}}} - \overbrace{dT_2}^{\text{Uninfected hepatocyte death rate}} - \overbrace{\beta T_2 V_2}^{\text{Infectivity rate}}, \\
\dot{I}_2 &= \overbrace{\beta T_2 V_2}^{\text{Virus production rate}} - \overbrace{\delta I_2}^{\text{Virus clearance rate}}, \\
\dot{V}_2 &= \overbrace{\rho I_2}^{\substack{\text{Viral movement rate from patch 1 to patch 2}\\ \text{Virus clearance rate}}} + \overbrace{\phi V_1}^{\text{Viral movement rate from patch 1 to patch 2}},
\end{aligned}
\tag{1.1}
$$

where $T_1 = T_1(t)$ denotes the uninfected hepatocytes in patch 1, $I_1 = I_1(t)$ denotes the infected hepatocytes in patch 1, $V_1 = V_1(t)$ represents the free HBV particles in patch 1, $T_2 = T_2(t)$ denotes the uninfected hepatocytes in patch 2, $I_2 = I_2(t)$ denotes the infected hepatocytes in patch 2 and $V_2 = V_2(t)$ represents the free HBV particles in patch 2. The infection in model (1.1) starts in patch 1 and then moves to patch 2 via the unidirectional viral transfer term ϕV_1.
In this work, we investigate the non-negativity and boundedness of the solutions and establish the global asymptotic stability of all equilibria. The global stability of all equilibrium points is established by Lyapunov method. Numerical simulation is conducted to support the theoritical results.

2. Basic qualitative properties

In this section, we investigate the fundamental properties of system (1.1). In particular, we establish the nonnegativity and boundedness of the solutions of the system to ensure the biological feasibility and well-posedness of the model.

Lemma 2.1. *Assuming that all initial conditions are nonnegative, the solutions of system (1.1) remain nonnegative and bounded.*

Proof. It follows that

$$\dot{T}_1 \mid_{T_1=0} = s_1 > 0, \quad \dot{I}_1 \mid_{I_1=0} = \beta T_1 V_1 \geq 0 \text{ for all } T_1, V_1 \geq 0,$$
$$\dot{V}_1 \mid_{V_1=0} = \rho I_1 \geq 0 \text{ for all } I_1 \geq 0,$$
$$\dot{T}_2 \mid_{T_2=0} = s_2 > 0, \quad \dot{I}_2 \mid_{I_2=0} = \beta T_2 V_2 \geq 0 \text{ for all } T_2, V_2 \geq 0,$$
$$\dot{V}_2 \mid_{V_2=0} = \rho I_2 + \phi V_1 \geq 0 \text{ for all } V_1, I_2 \geq 0.$$

This ensures that, $(T_1(t), I_1(t), V_1(t), T_2(t), I_2(t), V_2(t)) \in \mathbb{R}^6_{\geq 0}$ for all $t \geq 0$ provided that $(T_1(0), I_1(0), V_1(0), T_2(0), I_2(0), V_2(0)) \in \mathbb{R}^6_{\geq 0}$ [26]. We now define

$$\Psi_1(t) = T_1(t) + I_1(t).$$

Then

$$\dot{\Psi}_1(t) = s_1 - dT_1(t) - \delta I_1(t) \leq s_1 - \eta_1 (T_1(t) + I_1(t)) = s_1 - \eta_1 \Psi_1(t),$$

where $\eta_1 = \min\{d, \delta\}$. Thus, $0 \leq \Psi_1(t) \leq \Delta_1$ if $\Psi_1(0) \leq \Delta_1$ for $t \geq 0$, where $\Delta_1 = \frac{s_1}{\eta_1}$. Since $T_1(t) \geq 0$ and $I_1(t) \geq 0$, we obtain $0 \leq T_1(t) \leq \Delta_1$ and $0 \leq I_1(t) \leq \Delta_1$ if $T_1(0) + I_1(0) \leq \Delta_1$ for $t \geq 0$. From the third equation of system (1.1), we obtain

$$\dot{V}_1(t) = \rho I_1(t) - (c + \phi) V_1(t) \leq \rho \Delta_1 - (c + \phi) V_1(t).$$

Therefore, $0 \leq V_1(t) \leq \frac{\rho \Delta_1}{c+\phi} = \Delta_2$ if $V_1(0) \leq \Delta_2$. Let us define

$$\Psi_2(t) = T_2(t) + I_2(t).$$

Then

$$\dot{\Psi}_2(t) = s_2 - dT_2(t) - \delta I_2(t) \leq s_2 - \eta_1 (T_2(t) + I_2(t)) = s_2 - \eta_1 \Psi_2(t).$$

Thus, $0 \leq \Psi_2(t) \leq \Delta_3$ if $\Psi_2(0) \leq \Delta_3$ for $t \geq 0$, where $\Delta_3 = \frac{s_2}{\eta_1}$. Since $T_2(t) \geq 0$ and $I_2(t) \geq 0$, we obtain $0 \leq T_2(t) \leq \Delta_3$ and $0 \leq I_2(t) \leq \Delta_3$ if $T_2(0) + I_2(0) \leq \Delta_3$ for $t \geq 0$. Now, from the last equation of system (1.1), we derive

$$\dot{V}_2(t) = \rho I_2(t) - cV_2(t) + \phi V_1(t) \leq \rho\Delta_3 + \phi\Delta_2 - cV_2(t).$$

Therefore, $0 \leq V_2(t) \leq \frac{\rho\Delta_3 + \phi\Delta_2}{c} = \Delta_4$ if $V_2(0) \leq \Delta_4$. Hence, all state variables of system (1.1) are nonnegative and bounded for all $t \geq 0$.

3. Equilibria and threshold analysis

In this section, we determine the equilibrium points of the model and derive the threshold conditions governing their existence and biological feasibility. Any equilibrium point $\Xi = (T_1, I_1, V_1, T_2, I_2, V_2)$ satisfies:

$$0 = s_1 - dT_1 - \beta T_1 V_1, \tag{3.1}$$

$$0 = \beta T_1 V_1 - \delta I_1, \tag{3.2}$$

$$0 = \rho I_1 - cV_1 - \phi V_1, \tag{3.3}$$

$$0 = s_2 - dT_2 - \beta T_2 V_2, \tag{3.4}$$

$$0 = \beta T_2 V_2 - \delta I_2, \tag{3.5}$$

$$0 = \rho I_2 - cV_2 + \phi V_1. \tag{3.6}$$

It is obvious that system (1.1) has an infection-free equilibrium, $\Xi^\star = \left(T_1^\star, 0, 0, T_2^\star, 0, 0\right)$, where

$$T_1^\star = \frac{s_1}{d}, \quad T_2^\star = \frac{s_2}{d}.$$

Now we apply the method of next generation matrix to derive the threshold parameters linked to the infection-free equilibrium. The infected state variables are taken to be (I_1, V_1, I_2, V_2). Evaluating these terms at the infection-free equilibrium $\Xi^\star$, the Jacobian matrices K and H are given, respectively, by

$$K = \begin{pmatrix} 0 & \beta T_1^\star & 0 & 0 \\ 0 & 0 & 0 & 0 \\ 0 & 0 & 0 & \beta T_2^\star \\ 0 & 0 & 0 & 0 \end{pmatrix}, \text{ and } H = \begin{pmatrix} \delta & 0 & 0 & 0 \\ -\rho & c+\phi & 0 & 0 \\ 0 & 0 & \delta & 0 \\ 0 & -\phi & -\rho & c \end{pmatrix}.$$

Therefore, the eigenvalues of the next generation matrix KH^{-1} are

$$0, \quad 0, \quad \frac{\beta\rho T_1^\star}{\delta(c+\phi)}, \quad \frac{\beta\rho T_2^\star}{c\delta}.$$

In addition, its spectral radius is

$$R_0 = r(KH^{-1}) = \max\left\{\frac{\beta\rho T_1^\star}{\delta(c+\phi)}, \frac{\beta\rho T_2^\star}{c\delta}\right\}.$$

Accordingly, the basic reproduction number of the full two-patch system (1.1) is defined as follows:

$$R_0 = \max\{R_1, R_2\},$$

where

$$R_1 = \frac{\beta\rho T_1^\star}{\delta\,(c+\phi)} = \frac{\beta\rho s_1}{d\delta\,(c+\phi)}, \text{ and } R_2 = \frac{\beta\rho T_2^\star}{c\delta} = \frac{\beta\rho s_2}{c\delta d}.$$

Here R_1 and R_2 represent the patch-specific threshold parameters. They will be retained as separate threshold parameters, since they are needed to distinguish between the feasibility conditions of the one-patch and two-patch infected equilibria.

The straightforward calculation finds that, in addition to $\Xi^\star$, system (3.1)-(3.6) admits the following two biologically relevant equilibria:

- One-patch infected equilibrium $\bar{\Xi} = (\bar{T}_1, 0, 0, \bar{T}_2, \bar{I}_2, \bar{V}_2)$, where

$$T_1^\star = \bar{T}_1 = \frac{s_1}{d}, \quad \bar{T}_2 = \frac{c\delta}{\beta\rho},$$
$$\bar{I}_2 = \frac{cd}{\beta\rho}\,(R_2 - 1), \quad \bar{V}_2 = \frac{d}{\beta}\,(R_2 - 1).$$

  We note that $\bar{I}_2 > 0$ and $\bar{V}_2 > 0$ if and only if $R_2 > 1$. Consequently, the one-patch infected equilibrium $\bar{\Xi}$ exists whenever $R_2 > 1$.

- Two-patch infected equilibrium, $\tilde{\Xi} = (\tilde{T}_1, \tilde{I}_1, \tilde{V}_1, \tilde{T}_2, \tilde{I}_2, \tilde{V}_2)$, where

$$\tilde{T}_1 = \frac{\delta\,(c+\phi)}{\beta\rho}, \quad \tilde{I}_1 = \frac{d\,(c+\phi)}{\beta\rho}\,(R_1 - 1),$$
$$\tilde{V}_1 = \frac{d}{\beta}\,(R_1 - 1), \quad \tilde{V}_2 = \frac{s_2 - dT_2}{\beta T_2}, \quad \tilde{I}_2 = \frac{s_2 - dT_2}{\delta}. \tag{3.7}$$

  We note that $\tilde{I}_1 > 0$ and $\tilde{V}_1 > 0$ if and only if $R_1 > 1$. In addition, $\tilde{V}_2 > 0$ and $\tilde{I}_2 > 0$, when $T_2 \in \left(0, \frac{s_2}{d}\right)$. Substituting from Eq. (3.7) into Eq. (3.6), we get the component T_2 satisfies the quadratic equation

$$AT_2^2 + BT_2 + C = 0,$$

  where

$$A = \rho\beta d,$$
$$B = -\rho\beta s_2 - c\delta d - \delta\phi d\,(R_1 - 1),$$
$$C = c\delta s_2.$$

  The roots are given by

$$T_2 = \frac{-B \pm \sqrt{B^2 - 4AC}}{2A}.$$

  Let us define a function $P(T_2)$ as:

$$P(T_2) = \rho\beta d T_2^2 - \left(\rho\beta s_2 + c\delta d + \delta\phi d\,(R_1 - 1)\right) T_2 + c\delta s_2,$$

we have

$$\begin{aligned} P(0) &= c\delta s_2 > 0, \\ P\left(\frac{s_2}{d}\right) &= \frac{\rho\beta s_2^2}{d} - \left(\rho\beta s_2 + c\delta d + \delta\phi d\left(R_1 - 1\right)\right)\frac{s_2}{d} + c\delta s_2, \\ &= -\delta\phi s_2\left(R_1 - 1\right) < 0. \end{aligned}$$

Thus, using the intermediate value theorem, there exists at a root $\tilde{T}_2 \in \left(0, \frac{s_2}{d}\right)$. Consequently

$$\tilde{V}_2 = \frac{s_2 - d\tilde{T}_2}{\beta T_2} > 0, \quad \tilde{I}_2 = \frac{s_2 - d\tilde{T}_2}{\delta} > 0.$$

Therefore, the two-patch infected equilibrium $\tilde{\Xi}$ exists whenever $R_1 > 1$.

4. Global stability analysis

The study of stability is fundamental in dynamical systems, since only stable states can be realized in experimental settings. In this section, we analyze the global asymptotic stability of the system's equilibrium points. This is carried out by constructing suitable Lyapunov functions [27] and applying the Lyapunov-LaSalle asymptotic stability theorem (L-LAST) [28]- [30]. Moreover, the arithmetic mean-geometric mean (AM-GM) inequality will be used, namely

$$\frac{1}{n}\sum_{i=1}^{n}\chi_i \geq \sqrt[n]{\prod_{i=1}^{n}\chi_i}, \qquad \chi_i \geq 0,\ i = 1, 2, ..., \tag{4.1}$$

we use the Volterra-type function

$$F(v) = v - 1 - \ln v, \ \ v > 0,$$

which satisfies $F(v) \geq 0$ and $F(1) = 0$.

Theorem 4.1. *If $R_0 < 1$, then $\Xi^\star$ is globally asymptotically stable (G.A.S).*

Proof. We construct a candidate Lyapunov function as follows:

$$\begin{aligned} L^\star\left(T_1, I_1, V_1, T_2, I_2, V_2\right) = &\frac{\phi}{(c+\phi)\left(1-R_1\right)}T_1^\star F\left(\frac{T_1}{T_1^\star}\right) + \frac{\phi}{(c+\phi)\left(1-R_1\right)}I_1 \\ &+ \frac{\delta\phi}{\rho\left(c+\phi\right)\left(1-R_1\right)}V_1 + T_2^\star F\left(\frac{T_2}{T_2^\star}\right) + I_2 + \frac{\delta}{\rho}V_2. \end{aligned}$$

It is seen that, $L^\star > 0$ for all $T_1, I_1, V_1, T_2, I_2, V_2 > 0$, and $L^\star(T_1^\star, 0, 0, T_2^\star, 0, 0) = 0$. We calculate $\frac{dL^\star}{dt}$ along the solutions of model (1.1) as:

$$\begin{aligned} \frac{dL^\star}{dt} = &\frac{\phi}{(c+\phi)\left(1-R_1\right)}\left(1 - \frac{T_1^\star}{T_1}\right)\dot{T}_1 + \frac{\phi}{(c+\phi)\left(1-R_1\right)}\dot{I}_1 + \frac{\delta\phi}{\rho\left(c+\phi\right)\left(1-R_1\right)}\dot{V}_1 \\ &+ \left(1 - \frac{T_2^\star}{T_2}\right)\dot{T}_2 + \dot{I}_2 + \frac{\delta}{\rho}\dot{V}_2. \end{aligned}$$

Substituting from system (1.1), we obtain

$$\frac{dL^\star}{dt} = \frac{\phi}{(c+\phi)(1-R_1)}\left(1-\frac{T_1^\star}{T_1}\right)(s_1 - dT_1 - \beta T_1 V_1) + \frac{\phi}{(c+\phi)(1-R_1)}(\beta T_1 V_1 - \delta I_1)$$
$$+ \frac{\delta\phi}{\rho(c+\phi)(1-R_1)}(\rho I_1 - cV_1 - \phi V_1) + \left(1-\frac{T_2^\star}{T_2}\right)(s_2 - dT_2 - \beta T_2 V_2) + \beta T_2 V_2$$
$$- \delta I_2 + \frac{\delta}{\rho}(\rho I_2 - cV_2 + \phi V_1).$$

Collecting terms, we get

$$\frac{dL^\star}{dt} = \frac{\phi}{(c+\phi)(1-R_1)}\left(1-\frac{T_1^\star}{T_1}\right)(s_1 - dT_1) + \left(1-\frac{T_2^\star}{T_2}\right)(s_2 - dT_2) + \frac{\delta c}{\rho}(R_2 - 1)V_2.$$

Using the equilibrium condition $s_1 = dT_1^\star$, $s_2 = dT_2^\star$, we get:

$$\frac{dL^\star}{dt} = -\frac{d\phi}{(c+\phi)(1-R_1)}\frac{(T_1 - T_1^\star)^2}{T_1} - d\frac{(T_2 - T_2^\star)^2}{T_2} + \frac{\delta c}{\rho}(R_2 - 1)V_2.$$

Since $\max\{R_1, R_2\} < 1$, then $R_1 < 1$ and $R_2 < 1$ and consequently, $\frac{dL^\star}{dt} \leq 0$ for all $T_1, I_1, V_1, T_2, I_2, V_2 > 0$. In addition $\frac{dL^\star}{dt} = 0$ when $T_1 = T_1^\star$, $T_2 = T_2^\star$ and $V_2 = 0$. The solutions of system (1.1) tend to the largest invariant set Υ_0' contained in $\Upsilon_0 = \left\{(T_1, I_1, V_1, T_2, I_2, V_2) : \frac{dL^\star}{dt} = 0\right\}$. The set Υ_0' includes elements such that $T_1(t) = T_1^\star$, $T_2(t) = T_2^\star$, and $V_2(t) = 0$. Then, $\dot{T}_1(t) = 0$ and $\dot{V}_2(t) = 0$. From the first equation of system (1.1) we have

$$0 = \dot{T}_1(t) = s_1 - dT_1^* - \beta T_1^* V_1(t),$$

which gives $V_1(t) = 0$ for all t. Then, $\dot{V}_1(t) = 0$. Moreover, from the third and last equations of system (1.1), we have

$$0 = \dot{V}_1(t) = \rho I_1(t), \text{ and } 0 = \dot{V}_2(t) = \rho I_2(t),$$

which imply $I_1(t) = I_2(t) = 0$ for all t. Thus, the largest invariant set contained in Υ_0 is $\{\Xi^\star\}$. Therefore, applying the Lyapunov-LaSalle asymptotic stability theorem (L-LAST) [28]- [30], we conclude that $\Xi^\star$ is G.A.S.

Theorem 4.2. *Suppose that $R_1 < 1 < R_2$, then $\bar{\Xi}$ is G.A.S.*

Proof. We define a Lyapunov function $\bar{L}$ as follows:

$$\bar{L}(T_1, I_1, V_1, T_2, I_2, V_2) = \frac{\phi}{(c+\phi)(1-R_1)}\bar{T}_1 F\left(\frac{T_1}{\bar{T}_1}\right) + \frac{\phi}{(c+\phi)(1-R_1)}I_1 + \frac{\delta\phi}{\rho(c+\phi)(1-R_1)}V_1$$
$$+ \bar{T}_2 F\left(\frac{T_2}{\bar{T}_2}\right) + \bar{I}_2 F\left(\frac{I_2}{\bar{I}_2}\right) + \frac{\delta}{\rho}\bar{V}_2 F\left(\frac{V_2}{\bar{V}_2}\right).$$

It is seen that, $\bar{L}(T_1, I_1, V_1, T_2, I_2, V_2) > 0$ for all $T_1, I_1, V_1, T_2, I_2, V_2 > 0$, and $\bar{L}(\bar{T}_1, 0, 0, \bar{T}_2, \bar{I}_2, \bar{V}_2) = 0$. We calculate $\frac{d\bar{L}}{dt}$ as:

$$\frac{d\bar{L}}{dt} = \frac{\phi}{(c+\phi)(1-R_1)}\left(1-\frac{\bar{T}_1}{T_1}\right)(s_1 - dT_1 - \beta T_1 V_1) + \frac{\phi}{(c+\phi)(1-R_1)}(\beta T_1 V_1 - \delta I_1)$$

$$+\frac{\delta\phi}{\rho\left(c+\phi\right)\left(1-R_1\right)}\left(\rho I_1-cV_1-\phi V_1\right)+\left(1-\frac{\bar{T}_2}{T_2}\right)\left(s_2-dT_2-\beta T_2V_2\right)$$
$$+\left(1-\frac{\bar{I}_2}{I_2}\right)\left(\beta T_2V_2-\delta I_2\right)+\frac{\delta}{\rho}\left(1-\frac{\bar{V}_2}{V_2}\right)\left(\rho I_2-cV_2+\phi V_1\right).$$

Collecting terms, we obtain

$$\begin{aligned}\frac{d\bar{L}}{dt}&=\frac{\phi}{\left(c+\phi\right)\left(1-R_1\right)}\left(1-\frac{\bar{T}_1}{T_1}\right)\left(s_1-dT_1\right)+\frac{\phi}{\left(c+\phi\right)\left(1-R_1\right)}\beta\bar{T}_1V_1\\&-\frac{\delta\phi}{\rho\left(1-R_1\right)}V_1+\left(1-\frac{\bar{T}_2}{T_2}\right)\left(s_2-dT_2\right)+\beta\bar{T}_2V_2-\beta T_2V_2\frac{\bar{I}_2}{I_2}\\&+\delta\bar{I}_2-\frac{\delta c}{\rho}V_2+\frac{\delta\phi}{\rho}V_1-\delta I_2\frac{\bar{V}_2}{V_2}+\frac{\delta c}{\rho}\bar{V}_2-\frac{\delta\phi}{\rho}V_1\frac{\bar{V}_2}{V_2},\\&=\frac{\phi}{\left(c+\phi\right)\left(1-R_1\right)}\left(1-\frac{\bar{T}_1}{T_1}\right)\left(s_1-dT_1\right)+\left(1-\frac{\bar{T}_2}{T_2}\right)\left(s_2-dT_2\right)+\beta\bar{T}_2V_2\\&-\beta T_2V_2\frac{\bar{I}_2}{I_2}+\delta\bar{I}_2-\frac{\delta c}{\rho}V_2-\delta I_2\frac{\bar{V}_2}{V_2}+\frac{\delta c}{\rho}\bar{V}_2-\frac{\delta\phi}{\rho}V_1\frac{\bar{V}_2}{V_2}.\end{aligned}$$

Using the equilibrium conditions for $\bar{\Xi}$:

$$s_1=d\bar{T}_1,\quad s_2=d\bar{T}_2+\beta\bar{T}_2\bar{V}_2,\quad \beta\bar{T}_2\bar{V}_2=\delta\bar{I}_2,\quad \rho\bar{I}_2=c\bar{V}_2,$$

we obtain

$$\begin{aligned}\frac{d\bar{L}}{dt}&=-\frac{d\phi}{\left(c+\phi\right)\left(1-R_1\right)}\frac{\left(T_1-\bar{T}_1\right)^2}{T_1}-d\frac{\left(T_2-\bar{T}_2\right)^2}{T_2}+\beta\bar{T}_2\bar{V}_2\left(1-\frac{\bar{T}_2}{T_2}\right)\\&-\beta\bar{T}_2\bar{V}_2\frac{T_2V_2\bar{I}_2}{\bar{T}_2\bar{V}_2I_2}+\beta\bar{T}_2\bar{V}_2-\beta\bar{T}_2\bar{V}_2\frac{I_2\bar{V}_2}{\bar{I}_2V_2}+\beta\bar{T}_2\bar{V}_2-\frac{\delta\phi}{\rho}V_1\frac{\bar{V}_2}{V_2}.\\&=-\frac{d\phi}{\left(c+\phi\right)\left(1-R_1\right)}\frac{\left(T_1-\bar{T}_1\right)^2}{T_1}-d\frac{\left(T_2-\bar{T}_2\right)^2}{T_2}-\frac{\delta\phi}{\rho}V_1\frac{\bar{V}_2}{V_2}\\&+\beta\bar{T}_2\bar{V}_2\left(3-\frac{\bar{T}_2}{T_2}-\frac{T_2V_2\bar{I}_2}{\bar{T}_2\bar{V}_2I_2}-\frac{I_2\bar{V}_2}{\bar{I}_2V_2}\right).\end{aligned}$$

Using inequality (4.1), we get:

$$3-\frac{\bar{T}_2}{T_2}-\frac{T_2V_2\bar{I}_2}{\bar{T}_2\bar{V}_2I_2}-\frac{I_2\bar{V}_2}{\bar{I}_2V_2}\leq 0.$$

If $R_1<1<R_2$, then $\frac{d\bar{L}}{dt}\leq 0$ for all $T_1,I_1,V_1,T_2,I_2,V_2>0$. In addition $\frac{d\bar{L}}{dt}=0$ when $T_1=\bar{T}_1$, $T_2=\bar{T}_2$, $I_2=\bar{I}_2$, $V_2=\bar{V}_2$ and $V_1=0$. The solutions of system (1.1) tend to the largest invariant set $\mathrm{Y}_1^{'}$ contained in $\mathrm{Y}_1=\left\{\left(T_1,I_1,V_1,T_2,I_2,V_2\right):\frac{d\bar{L}}{dt}=0\right\}$. On this invariant set, since $V_1\left(t\right)=0$ for all t we have $\dot{V}_1\left(t\right)=0$. Then from the third equation of system (1.1), we have

$$0=\dot{V}_1\left(t\right)=\rho I_1\left(t\right)\Longrightarrow I_1(t)=0,\text{ for all }t.$$

Therefore, $\mathrm{Y}_1^{'}=\{\bar{\Xi}\}$. Consequently, by applying the L-LAST, we conclude the $\bar{\Xi}$ is G.A.S.

Assumption. We impose the following assumption for the global stability of the two-patch infected equilibrium:

$$\left(V_2-\tilde{V}_2\right)\left(\frac{V_1}{V_2}-\frac{\tilde{V}_1}{\tilde{V}_2}\right)\leq 0, \qquad t\geq 0. \tag{A}$$

This assumption reflects a compensatory effect between the viral load in patch 2 and the relative distribution of the virus between the two patches due to inter-patch transport.

Theorem 4.3. *If assumption (A) holds and $R_1>1$, then $\tilde{\Xi}$ is G.A.S.*

Proof. Consider a function $\tilde{L}$ as:

$$\begin{aligned}\tilde{L}\left(T_1,I_1,V_1,T_2,I_2,V_2\right)=\frac{\phi}{c+\phi}\left(\tilde{T}_1F\left(\frac{T_1}{\tilde{T}_1}\right)+\tilde{I}_1F\left(\frac{I_1}{\tilde{I}_1}\right)+\frac{\delta}{\rho}\tilde{V}_1F\left(\frac{V_1}{\tilde{V}_1}\right)\right)\\ +\tilde{T}_2F\left(\frac{T_2}{\tilde{T}_2}\right)+\tilde{I}_2F\left(\frac{I_2}{\tilde{I}_2}\right)+\frac{\delta}{\rho}\tilde{V}_2F\left(\frac{V_2}{\tilde{V}_2}\right).\end{aligned}$$

We obsrve that, $\tilde{L}\left(T_1,I_1,V_1,T_2,I_2,V_2\right)>0$ for all $T_1,I_1,V_1,T_2,I_2,V_2>0$, and $\tilde{L}\left(\tilde{T}_1,\tilde{I}_1,\tilde{V}_1,\tilde{T}_2,\tilde{I}_2,\tilde{V}_2\right)=0$. We calculate $\frac{d\tilde{L}}{dt}$ as:

$$\begin{aligned}\frac{d\tilde{L}}{dt}&=\frac{\phi}{c+\phi}\left(1-\frac{\tilde{T}_1}{T_1}\right)\left(s_1-dT_1-\beta T_1V_1\right)+\frac{\phi}{c+\phi}\left(1-\frac{\tilde{I}_1}{I_1}\right)\left(\beta T_1V_1-\delta I_1\right)\\ &+\frac{\delta\phi}{\rho\left(c+\phi\right)}\left(1-\frac{\tilde{V}_1}{V_1}\right)\left(\rho I_1-\left(c+\phi\right)V_1\right)+\left(1-\frac{\tilde{T}_2}{T_2}\right)\left(s_2-dT_2-\beta T_2V_2\right)\\ &+\left(1-\frac{\tilde{I}_2}{I_2}\right)\left(\beta T_2V_2-\delta I_2\right)+\frac{\delta}{\rho}\left(1-\frac{\tilde{V}_2}{V_2}\right)\left(\rho I_2-cV_2+\phi V_1\right).\end{aligned} \tag{4.2}$$

Then simplifying Eq. (4.2), we get

$$\begin{aligned}\frac{d\tilde{L}}{dt}&=\frac{\phi}{c+\phi}\left(1-\frac{\tilde{T}_1}{T_1}\right)\left(s_1-dT_1\right)+\frac{\phi}{c+\phi}\beta\tilde{T}_1V_1-\frac{\phi}{c+\phi}\beta T_1V_1\frac{\tilde{I}_1}{I_1}+\frac{\delta\phi}{c+\phi}\tilde{I}_1\\ &-\frac{\delta\phi}{c+\phi}I_1\frac{\tilde{V}_1}{V_1}+\frac{\delta\phi}{\rho}\tilde{V}_1+\left(1-\frac{\tilde{T}_2}{T_2}\right)\left(s_2-dT_2\right)+\beta\tilde{T}_2V_2-\beta T_2V_2\frac{\tilde{I}_2}{I_2}+\delta\tilde{I}_2\\ &-\frac{\delta c}{\rho}V_2-\delta I_2\frac{\tilde{V}_2}{V_2}+\frac{\delta c}{\rho}\tilde{V}_2-\frac{\delta\phi}{\rho}V_1\frac{\tilde{V}_2}{V_2}.\end{aligned}$$

Using the equilibrium conditions for $\tilde{\Xi}$:

$$\begin{aligned}s_1&=d\tilde{T}_1+\beta\tilde{T}_1\tilde{V}_1,\quad \beta\tilde{T}_1\tilde{V}_1=\delta\tilde{I}_1=\frac{\delta\left(c+\phi\right)}{\rho}\tilde{V}_1,\quad \rho\tilde{I}_1=\left(c+\phi\right)\tilde{V}_1,\\ s_2&=d\tilde{T}_2+\beta\tilde{T}_2\tilde{V}_2,\quad \beta\tilde{T}_2\tilde{V}_2=\delta\tilde{I}_2=\frac{\delta c}{\rho}\tilde{V}_2-\frac{\delta\phi}{\rho}\tilde{V}_1,\quad \rho\tilde{I}_2=c\tilde{V}_2-\phi\tilde{V}_1,\end{aligned}$$

we obtain

$$\begin{aligned}\frac{d\tilde{L}}{dt}&=\frac{\phi}{c+\phi}\left(1-\frac{\tilde{T}_1}{T_1}\right)\left(d\tilde{T}_1-dT_1\right)+\frac{\phi}{c+\phi}\left(1-\frac{\tilde{T}_1}{T_1}\right)\beta\tilde{T}_1\tilde{V}_1+\frac{\delta\phi}{\rho}V_1-\frac{\phi}{c+\phi}\beta\tilde{T}_1\tilde{V}_1\frac{T_1V_1\tilde{I}_1}{\tilde{T}_1\tilde{V}_1I_1}\\ &+\frac{\phi}{c+\phi}\beta\tilde{T}_1\tilde{V}_1-\frac{\phi}{c+\phi}\beta\tilde{T}_1\tilde{V}_1\frac{I_1\tilde{V}_1}{\tilde{I}_1V_1}+\frac{\phi}{c+\phi}\beta\tilde{T}_1\tilde{V}_1+\left(1-\frac{\tilde{T}_2}{T_2}\right)\left(d\tilde{T}_2-dT_2\right)+\beta\tilde{T}_2\tilde{V}_2\left(1-\frac{\tilde{T}_2}{T_2}\right)\end{aligned}$$

$$+\beta\tilde{T}_2V_2-\beta\tilde{T}_2\tilde{V}_2\frac{T_2V_2\tilde{I}_2}{\tilde{T}_2\tilde{V}_2I_2}+\beta\tilde{T}_2\tilde{V}_2-\frac{\delta c}{\rho}V_2-\beta\tilde{T}_2\tilde{V}_2\frac{I_2\tilde{V}_2}{\tilde{I}_2V_2}+\beta\tilde{T}_2\tilde{V}_2+\frac{\delta\phi}{\rho}\tilde{V}_1-\frac{\delta\phi}{\rho}V_1\frac{\tilde{V}_2}{V_2},$$

$$=-\frac{d\phi}{c+\phi}\frac{\left(T_1-\tilde{T}_1\right)^2}{T_1}+\frac{\phi}{c+\phi}\beta\tilde{T}_1\tilde{V}_1\left(3-\frac{\tilde{T}_1}{T_1}-\frac{T_1V_1\tilde{I}_1}{\tilde{T}_1\tilde{V}_1I_1}-\frac{I_1\tilde{V}_1}{\tilde{I}_1V_1}\right)-d\frac{\left(T_2-\tilde{T}_2\right)^2}{T_2}$$

$$+\beta\tilde{T}_2\tilde{V}_2\left(3-\frac{\tilde{T}_2}{T_2}-\frac{T_2V_2\tilde{I}_2}{\tilde{T}_2\tilde{V}_2I_2}-\frac{I_2\tilde{V}_2}{\tilde{I}_2V_2}\right)+\frac{\delta\phi}{\rho}\left(V_1-\tilde{V}_1\frac{V_2}{\tilde{V}_2}+\tilde{V}_1-V_1\frac{\tilde{V}_2}{V_2}\right),$$

$$=-d\left(\frac{\phi}{c+\phi}\frac{\left(T_1-\tilde{T}_1\right)^2}{T_1}+\frac{\left(T_2-\tilde{T}_2\right)^2}{T_2}\right)+\frac{\phi}{c+\phi}\beta\tilde{T}_1\tilde{V}_1\left(3-\frac{\tilde{T}_1}{T_1}-\frac{T_1V_1\tilde{I}_1}{\tilde{T}_1\tilde{V}_1I_1}-\frac{I_1\tilde{V}_1}{\tilde{I}_1V_1}\right)$$

$$+\beta\tilde{T}_2\tilde{V}_2\left(3-\frac{\tilde{T}_2}{T_2}-\frac{T_2V_2\tilde{I}_2}{\tilde{T}_2\tilde{V}_2I_2}-\frac{I_2\tilde{V}_2}{\tilde{I}_2V_2}\right)+\frac{\delta\phi}{\rho}\left(V_2-\tilde{V}_2\right)\left(\frac{V_1}{V_2}-\frac{\tilde{V}_1}{\tilde{V}_2}\right).$$

Using inequality (4.1) and Assumption (A), we get $\frac{d\tilde{L}}{dt}\leq 0$ for all $T_1,V_1,I_1,T_2,I_2,V_2>0$. In addition $\frac{d\tilde{L}}{dt}=0$ when $T_1=\tilde{T}_1,I_1=\tilde{I}_1,V_1=\tilde{V}_1,T_2=\tilde{T}_2,I_2=\tilde{I}_2$, and $V_2=\tilde{V}_2$. The solutions of system (1.1) tend to the largest invariant set $\Upsilon_2^{'}$ contained in $\Upsilon_2=\left\{(T_1,I_1,V_1,T_2,I_2,V_2):\frac{d\tilde{L}}{dt}=0\right\}$. Therefore, $\Upsilon_2^{'}=\left\{\tilde{\Xi}\right\}$, and applying L-LAST, we obtain that $\tilde{\Xi}$ is G.A.S.

Based on the results obtaoned above, we summarize the existence and global stability conditions for all equilibrium points in Table 1.

TABLE 1. Criteria for existence and global stability of equilibrium points.

Equilibrium point	Existence condition	Global stability condition
$\Xi^*=(T_1^*,0,0,T_2^*,0,0)$	Always exists	$\max\{R_1,R_2\}<1$
$\bar{\Xi}=(\bar{T}_1,0,0,\bar{T}_2,\bar{I}_2,\bar{V}_2)$	$R_2>1$	$R_1<1<R_2$
$\tilde{\Xi}=(\tilde{T}_1,\tilde{I}_1,\tilde{V}_1,\tilde{T}_2,\tilde{I}_2,\tilde{V}_2)$	$R_1>1$	$R_1>1$ and Assumption (A) holds

5. NUMERICAL SIMULATIONS

This section is devoted to carrying out numerical simulations to support the theoretical outcomes shown in the previous section. Unless otherwise specified, the numerical simulations are conducted using the parameter values provided in Table 2.

TABLE 2. Model parameters.

Parameter	Description	Value	Source
s_1	Hepatocyte production rate in patch 1	3.4	[21]
s_2	Hepatocyte production rate in patch 2	6.12	[21]
d	Uninfected hepatocyte death rate	0.01	[21], [31], [32], [33]
β	Infectivity rate	Varied	Assumed
δ	Infected hepatocyte death rate	0.01	[21]
ρ	Virus production rate	Varied	Assumed
c	Virus clearance rate	4.4	[21], [34]
ϕ	Viral movement rate from patch 1 to patch 2	0.1	[21]

5.1. **Stability of the equilibria.** In this subsection, we further support the global stability results established in Theorems 4.1-4.3 by showing that, under different parameter regimes, the solutions of system (1.1) converge to one of the three equilibrium states. To achieve this, system (1.1) is solved using different initial conditions as outlined below:

$$\begin{aligned} T_1(0) &= 20 + 30k, & I_1(0) &= 50 - 5k, \\ V_1(0) &= 0.01 + 0.03k, & T_2(0) &= 50 + 80k, \\ I_2(0) &= 1 + 0.01k, & V_2(0) &= 0.01 + 0.08k, \qquad k = 1, 2, ..., 6. \end{aligned}$$

Selecting appropriate values of β and ρ yields the following three situations:

Situation 1 (Stability of Ξ^*): When $\beta = 0.1$ and $\rho = 0.0001$, we obtain $R_2 = 0.1391 < 1$ and $R_1 = 0.0756 < 1$. This gives $R_0 = 0.1391$. As shown in Figure 2, the system trajectories converge to the infection-free equilibrium $\Xi^* = (340, 0, 0, 612, 0, 0)$ for various initial conditions. This confirms that Ξ^* is G.A.S, consistent with Theorem 4.1. In this case, HBV particles are eliminated from both patches.

Situation 2 (Stability of $\bar{\Xi}$): For $\beta = 0.01$ and $\rho = 0.01$, the reproduction numbers are $R_2 = 1.3909 > 1$ and $R_1 = 0.7556 < 1$. In this case, the one-patch infected equilibrium $\bar{\Xi}$ exists and is given by $\bar{\Xi} = (340, 0, 0, 440, 172, 0.391)$. Figure 3 illustrates that all trajectories converge to this equilibrium point regardless of the initial conditions, which aligns with the result of Theorem 4.2. In this scenario, the virus persists only in the second patch.

Situation 3 (Stability of $\tilde{\Xi}$): By selecting $\beta = 0.1$ and $\rho = 0.01$, we obtain $R_1 = 7.556 > 1$ and Assumption (A) holds. Numerical simulations confirm the existence of the two-patch infected equilibrium $\tilde{\Xi} = (45, 295, 0.656, 43.498, 568.502, 1.307)$. As shown in Figure 4, the system trajectories converge to $\tilde{\Xi}$ from all tested initial conditions. These results are consistent with the theoretical findings established in Theorem 4.3. In this case, the virus persists in both patches.

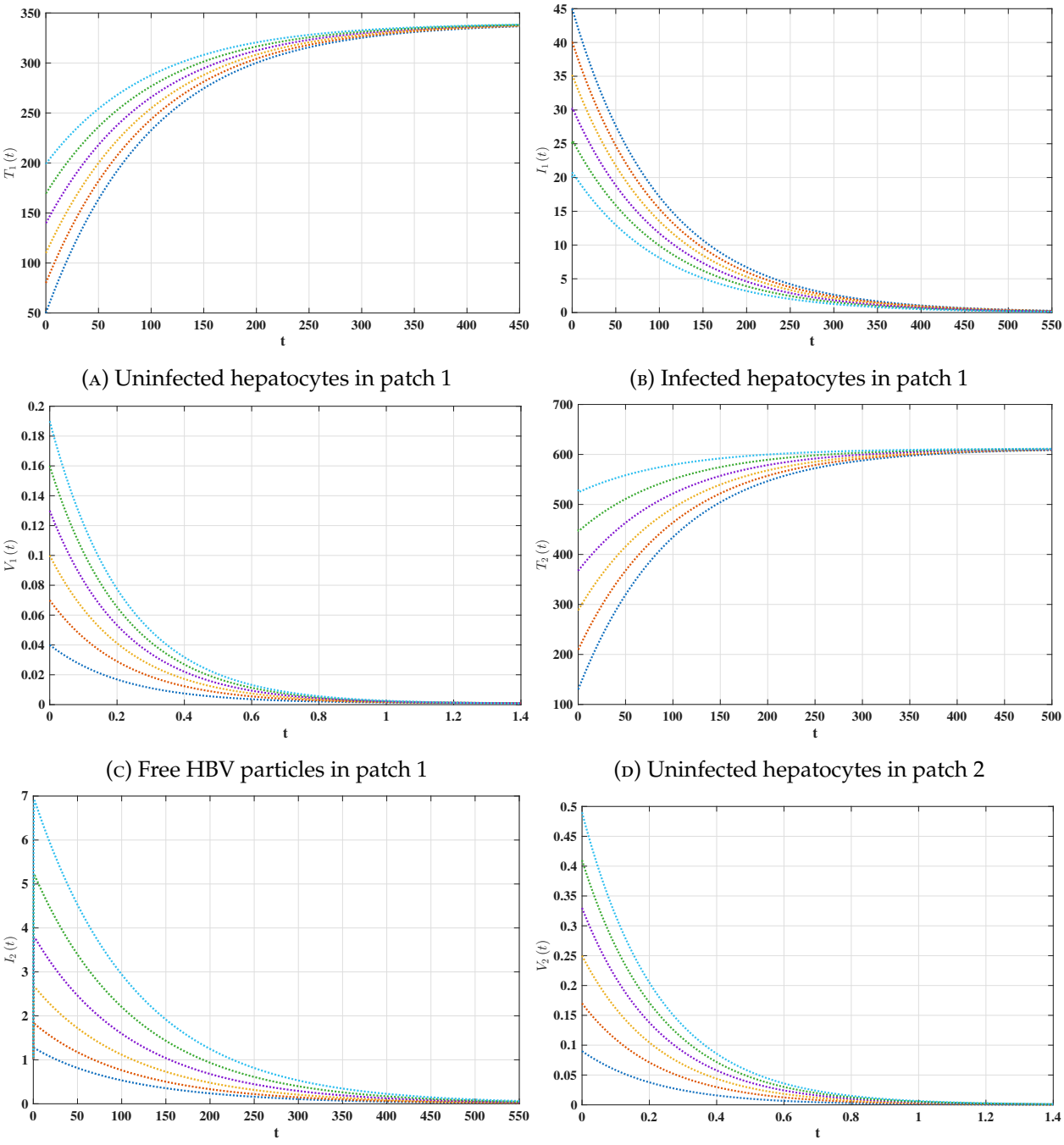

(A) Uninfected hepatocytes in patch 1

(B) Infected hepatocytes in patch 1

(C) Free HBV particles in patch 1

(D) Uninfected hepatocytes in patch 2

(E) Infected hepatocytes in patch 2

(F) Free HBV particles in patch 2

FIGURE 2. The solutions of system (1.1) converge to $\Xi^* = (340, 0, 0, 612, 0, 0)$ when $R_0 < 1$ (Situation 1).

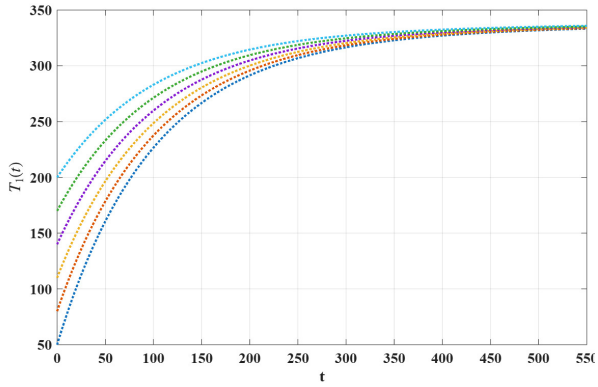

(A) Uninfected hepatocytes in patch 1

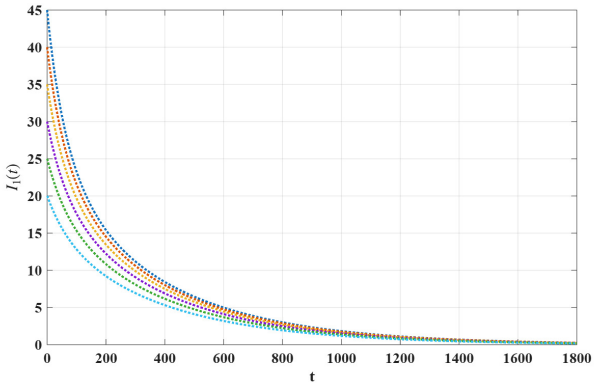

(B) Infected hepatocytes in patch 1

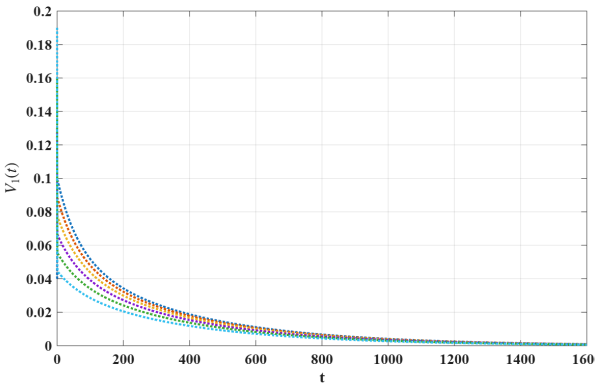

(C) Free HBV particles in patch 1

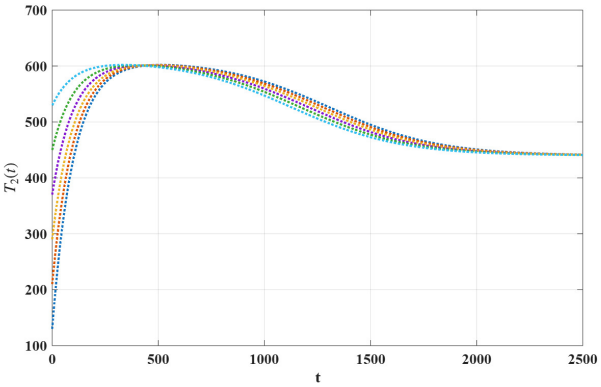

(D) Uninfected hepatocytes in patch 2

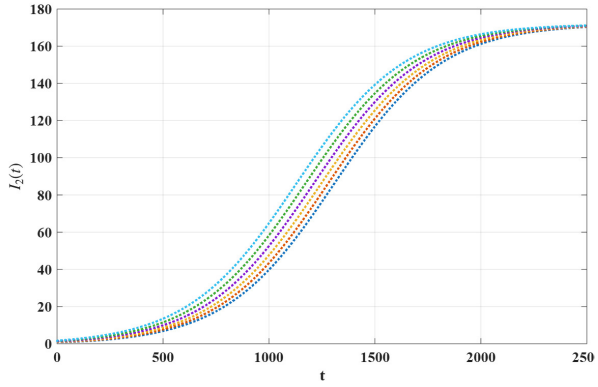

(E) Infected hepatocytes in patch 2

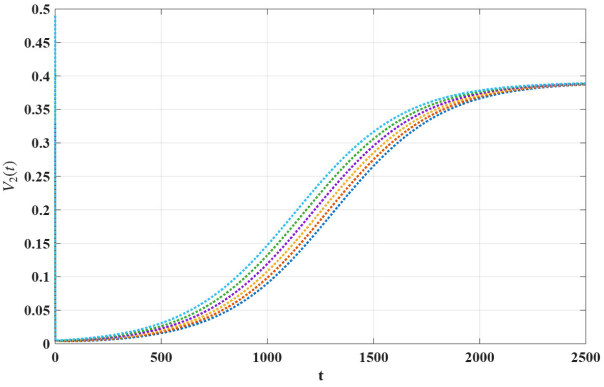

(F) Free HBV particles in patch 2

FIGURE 3. The solutions of system (1.1) converge to $\bar{\Xi} = (340, 0, 0, 440, 172, 0.391)$ when $R_1 < 1 < R_2$ (Situation 2).

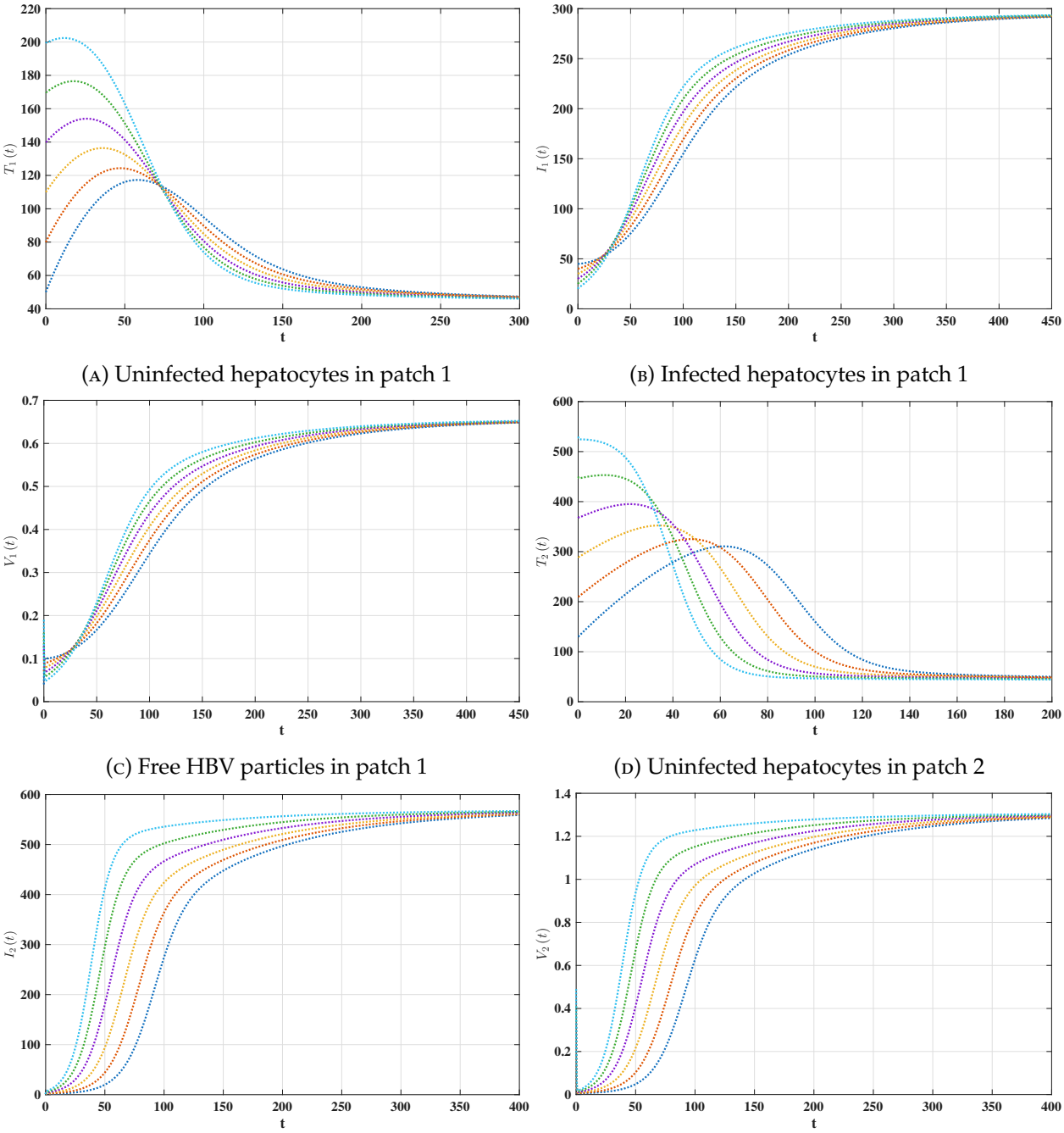

(A) Uninfected hepatocytes in patch 1

(B) Infected hepatocytes in patch 1

(C) Free HBV particles in patch 1

(D) Uninfected hepatocytes in patch 2

(E) Infected hepatocytes in patch 2

(F) Free HBV particles in patch 2

FIGURE 4. The solutions of system (1.1) converge to $\tilde{\Xi} = (45, 295, 0.656, 43.498, 568.502, 1.307)$ when $R_1 > 1$ and assumption (A) holds (Situation 3).

6. Sensitivity analysis

Sensitivity analysis is a fundamental tool in biological modeling, as it provides insight into how variations in model parameters influence system behavior, thereby improving understanding of the model structure [35]. It is particularly effective for determining the parameters that most strongly govern the dynamics of the system [36]. Several methods exist for investigating parameter influence in biological systems, including direct differentiation, Latin hypercube sampling, and approaches based on system linearization followed by solution of the resulting equations [37], [38].

In this work, a derivative-based sensitivity analysis is employed for system (1.1). Sensitivities are computed analytically using partial derivatives with respect to the model parameters. The analysis focuses on the threshold quantities R_1 and R_2, as they play a key role in determining the stability of the disease-free equilibrium Ξ^*.

The normalized forward sensitivity index is defined as

$$\Lambda_{\alpha}^{R_i} = \frac{\partial R_i}{\partial \alpha} \cdot \frac{\alpha}{R_i}, \quad i = 1, 2, \tag{6.1}$$

where α represents a model parameter. The resulting sensitivity indices for R_1 and R_2, computed using Eq. (6.1), are summarized in Table 3 and illustrated in Figure 5.

Table 3. Sensitivity index of R_1 and R_2

Parameter α	Sensitivity index $\Lambda_{\alpha}^{R_1}$	Parameter α	Sensitivity index $\Lambda_{\alpha}^{R_2}$
β	1	β	1
ρ	1	ρ	1
s_1	1	s_2	1
d	-1	d	-1
δ	-1	δ	-1
c	-0.977778	c	-1
ϕ	-0.022222		

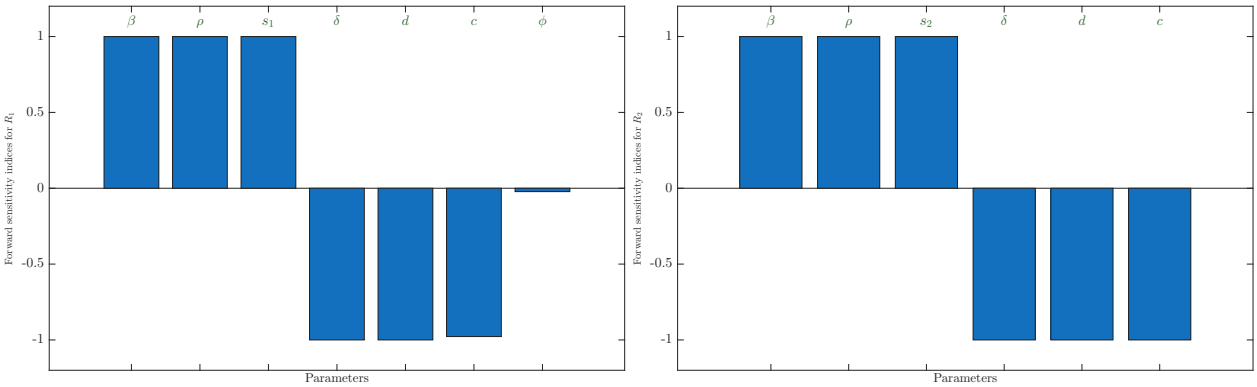

(A) Sensitivity analysis of R_1

(B) Sensitivity analysis of R_2

Figure 5. Forward sensitivity analysis of the parameters on R_1 and R_2.

6.1. **Sensitivity indices $\Lambda_{\alpha}^{R_1}$.** The computed sensitivity indices reveal the following results:

- The parameters β, ρ and s_1 possess positive sensitivity indices, indicating a direct relationship with R_1. Consequently, any increase (or decrease) in these parameters leads to a proportional rise (or fall) in R_1, thereby promoting infection propagation. These parameters also show the highest positive sensitivity values, where a 10% variation in each of β, ρ, or s_1 produces an equivalent 10% change in R_1.
- Conversely, δ, d, c, and ϕ exhibit negative sensitivity indices, indicating an inverse effect on R_1. Thus, increasing (or decreasing) these parameters results in a reduction (or increase) in R_1, thereby suppressing infection spread. Among them, δ and d have the most pronounced negative effects, followed by c, while ϕ has a relatively minor influence. Quantitatively, a 10% change in δ or d induces a 10% change in R_1 in the opposite direction, whereas a similar variation in c leads to an approximately 9.978% opposite change. In contrast, ϕ produces only a small effect of about 0.22%.

6.2. **Sensitivity indices $\Lambda_{\alpha}^{R_2}$.** The analysis of sensitivity indices for R_2 leads to the following observations:

- The parameters β, ρ, and s_2 have positive sensitivity indices, indicating a direct positive effect on R_2. Thus, an increase (or decrease) in any of these parameters leads to a corresponding increase (or decrease) in R_2, thereby enhancing the potential for infection spread. Among these, β, ρ, and s_2 exhibit the strongest positive influence. In particular, a 10% increase (or decrease) in any of these parameters results in an equivalent 10% increase (or decrease) in R_2.
- In contrast, δ, d, and c have negative sensitivity indices, reflecting an inverse relationship with R_2. Accordingly, increases (or decreases) in these parameters reduce (or raise) R_2, thereby limiting disease spread. A 10% variation in any of these parameters produces an equivalent 10% change in R_2 in the opposite direction.

7. Discussion

We extended the study of within-host mathematical models of HBV infection that account for the abnormal nodular structure of the liver, as reported in some previous works [21]. We analyzed the fundamental and global properties of the model and showed that the system admits three equilibrium points, whose existence and global stability are determined by two threshold parameters (R_1, R_2). The following results were established:

The infection-free equilibrium Ξ^* exists for all parameter values and is G.A.S., whenever $\max\{R_1, R_2\} < 1$. Under these conditions, viral clearance occurs in both patch 1 and patch 2. From a control viewpoint, maintaining $R_1 < 1$ and $R_2 < 1$ provides an effective control strategy, which can be implemented by decreasing the parameters β or ρ. Let $\epsilon_1 \in [0, 1]$ and $\epsilon_2 \in [0, 1]$ denote the efficacy of antiviral therapies against HBV, aimed at inhibiting HBV replication [39], [40]. Then, the transmission rate β is adjusted to $(1 - \epsilon_1)\beta$ and $(1 - \epsilon_2)\beta$, respectively. Consequently, R_1 and

R_2 are modified to:

$$R_1(\epsilon_1) = \frac{(1-\epsilon_1)\beta\rho T_1^\star}{\delta(c+\phi)},\ R_2(\epsilon_2) = \frac{(1-\epsilon_2)\beta\rho T_2^\star}{c\delta}.$$

To ensure $R_1 < 1$ and $R_2 < 1$, the effectiveness parameters ϵ_1 and ϵ_2 must satisfy:

$$\epsilon_1^{\min} < \epsilon_1 \leq 1,\ \ \epsilon_2^{\min} < \epsilon_2 \leq 1,$$

where:

$$\epsilon_1^{\min} = \max\left\{0, 1 - \frac{1}{R_1(0)}\right\},\ \ \epsilon_2^{\min} = \max\left\{0, 1 - \frac{1}{R_2(0)}\right\}.$$

Thus, complete clearance of HBV may be achieved by applying antiviral drug therapies with sufficient efficacy.

8. Conclusions

Mathematical modeling is a key tool for describing the complex dynamics of biological systems. In this study, we analyzed the global asymptotic stability of a two-patch within-host HBV infection model. The model is represented by a six-dimensional system of nonlinear ordinary differential equations (ODEs) that captures the interactions among uninfected hepatocytes (patch 1), infected hepatocytes (patch 1), free HBV virions (patch 1), uninfected hepatocytes (patch 2), infected hepatocytes (patch 2), and free HBV virions (patch 2).

We initially analyzed the non-negativity and boundedness of its solutions. Subsequently, we derived the equilibrium points and characterized their existence using the basic reproduction numbers R_1 and R_2. The global stability of all equilibria was established through Lyapunov function techniques together with the Lyapunov–LaSalle invariance principle. Numerical simulations were conducted, which confirmed and supported the theoretical findings. Finally, sensitivity analysis identifies the key parameters influencing viral persistence.

The proposed model and its analysis reveal three main biological states, (i) clearance of HBV particles in both patches, (ii) presence of the virus in only one-patch, and (iii) coexistence of the virus in both patches.

The model developed in this study can be further improved by (i) using real data to obtain accurate parameter estimates, (ii) investigating the effects of time delays during infection or virus production, and (iii) including the role of immune response. These directions require further investigation and are left for future work.

Acknowledgements: The authors gratefully acknowledge the Deanship of Scientific Research (DSR) at King Abdulaziz University, Jeddah, Saudi Arabia, for funding this project under grant No. (IPP: 331-130-2026) and for providing technical support.

Conflicts of Interest: The authors declare that there are no conflicts of interest regarding the publication of this paper.

References

[1] World Health Organization, Hepatitis, Global Health Observatory, 2022. https://www.who.int/data/gho/data/themes/chronic-viral-hepatitis.

[2] M.G. Mavilia, G.Y. Wu, HBV-HCV Coinfection: Viral Interactions, Management, and Viral Reactivation, J. Clin. Transl. Hepatol. 6 (2018), 296–305. https://doi.org/10.14218/JCTH.2018.00016.

[3] Q. Maqsood, A. Sumrin, M. Iqbal, S. Younas, N. Hussain, M. Mahnoor, A. Wajid, Hepatitis C Virus/Hepatitis B Virus Coinfection: Current Prospectives, Antivir. Ther. 28 (2023), 13596535231189643. https://doi.org/10.1177/13596535231189643.

[4] G. Raimondo, G. Cacciamo, C. Saitta, Hepatitis B Virus and Hepatitis C Virus Co-infection: Additive Players in Chronic Liver Disease?, Ann. Hepatol. 4 (2005), 100–106. https://doi.org/10.1016/S1665-2681(19)32072-1.

[5] L.G. Guidotti, F.V. Chisari, Immunobiology and Pathogenesis of Viral Hepatitis, Annu. Rev. Pathol. Mech. Dis. 1 (2006), 23–61. https://doi.org/10.1146/annurev.pathol.1.110304.100230.

[6] W.M. Lee, Hepatitis B Virus Infection, N. Engl. J. Med. 337 (1997), 1733–1745. https://doi.org/10.1056/nejm199712113372406.

[7] S. Locarnini, A. Hatzakis, D.-S. Chen, A. Lok, Strategies to Control Hepatitis B: Public Policy, Epidemiology, Vaccine and Drugs, J. Hepatol. 62 (2015), S76–S86. https://doi.org/10.1016/j.jhep.2015.01.018.

[8] G. Dusheiko, Treatment of HBeAg Positive Chronic Hepatitis B: Interferon or Nucleoside Analogues, Liver Int. 33 (2013), 137–150. https://doi.org/10.1111/liv.12078.

[9] J.-M. Pawlotsky, New Hepatitis B Drug Development Disillusions: Time to Reset?, Lancet Gastroenterol. Hepatol. 8 (2023), 192–197. https://doi.org/10.1016/S2468-1253(22)00341-7.

[10] M.A. Nowak, S. Bonhoeffer, A.M. Hill, R. Boehme, H.C. Thomas, H. McDade, Viral Dynamics in Hepatitis B Virus Infection, Proc. Natl. Acad. Sci. U.S.A. 93 (1996), 4398–4402. https://doi.org/10.1073/pnas.93.9.4398.

[11] M.A. Nowak, C.R.M. Bangham, Population Dynamics of Immune Responses to Persistent Viruses, Science 272 (1996), 74–79. https://doi.org/10.1126/science.272.5258.74.

[12] N. Yousfi, K. Hattaf, A. Tridane, Modeling the Adaptive Immune Response in HBV Infection, J. Math. Biol. 63 (2011), 933–957. https://doi.org/10.1007/s00285-010-0397-x.

[13] K. Manna, S.P. Chakrabarty, Chronic Hepatitis B Infection and HBV DNA-Containing Capsids: Modeling and Analysis, Commun. Nonlinear Sci. Numer. Simul. 22 (2015), 383–395. https://doi.org/10.1016/j.cnsns.2014.08.036.

[14] K. Manna, Global Properties of a HBV Infection Model with HBV DNA-Containing Capsids and CTL Immune Response, Int. J. Appl. Comput. Math. 3 (2017), 2323–2338. https://doi.org/10.1007/s40819-016-0205-4.

[15] S. Harroudi, A. Meskaf, K. Allali, Modelling the Adaptive Immune Response in HBV Infection Model with HBV DNA-Containing Capsids, Differ. Equ. Dyn. Syst. 31 (2023), 371–393. https://doi.org/10.1007/s12591-020-00549-1.

[16] R. Xu, Z. Ma, An HBV Model with Diffusion and Time Delay, J. Theor. Biol. 257 (2009), 499–509. https://doi.org/10.1016/j.jtbi.2009.01.001.

[17] Y. Geng, J. Xu, J. Hou, Discretization and Dynamic Consistency of a Delayed and Diffusive Viral Infection Model, Appl. Math. Comput. 316 (2018), 282–295. https://doi.org/10.1016/j.amc.2017.08.041.

[18] A.M. Elaiw, A.D. Al Agha, Global Dynamics of a General Diffusive HBV Infection Model with Capsids and Adaptive Immune Response, Adv. Differ. Equ. 2019 (2019), 519. https://doi.org/10.1186/s13662-019-2448-y.

[19] N. Roehlen, E. Crouchet, T.F. Baumert, Liver Fibrosis: Mechanistic Concepts and Therapeutic Perspectives, Cells 9 (2020), 875. https://doi.org/10.3390/cells9040875.

[20] L. Yuan, J. Jiang, X. Liu, Y. Zhang, L. Zhang, J. Xin, K. Wu, X. Li, J. Cao, X. Guo, D. Shi, J. Li, L. Jiang, S. Sun, T. Wang, W. Hou, T. Zhang, H. Zhu, J. Zhang, Q. Yuan, T. Cheng, J. Li, N. Xia, HBV Infection-Induced Liver Cirrhosis Development in Dual-Humanised Mice with Human Bone Mesenchymal Stem Cell Transplantation, Gut 68 (2019), 2044–2056. https://doi.org/10.1136/gutjnl-2018-316091.

[21] K. Castellano, O. Saucedo, S.M. Ciupe, Investigation of a Two-Patch Within-Host Model of Hepatitis B Viral Infection, Bull. Math. Biol. 87 (2025), 181. https://doi.org/10.1007/s11538-025-01555-6.

[22] BioRender. https://www.biorender.com.

[23] D. Schuppan, Y.O. Kim, Evolving Therapies for Liver Fibrosis, J. Clin. Invest. 123 (2013), 1887–1901. https://doi.org/10.1172/JCI66028.

[24] M.A. Nowak, R.M. May, Virus Dynamics: Mathematical Principles of Immunology and Virology, Oxford University Press, 2000.

[25] A.S. Perelson, R.M. Ribeiro, Modeling the Within-Host Dynamics of HIV Infection, BMC Biol. 11 (2013), 96. https://doi.org/10.1186/1741-7007-11-96.

[26] H.L. Smith, P. Waltman, The Theory of the Chemostat, Cambridge University Press, 1995. https://doi.org/10.1017/CBO9780511530043.

[27] A. Korobeinikov, Global Properties of Basic Virus Dynamics Models, Bull. Math. Biol. 66 (2004), 879–883. https://doi.org/10.1016/j.bulm.2004.02.001.

[28] E.A. Barbashin, Introduction to the Theory of Stability, Wolters-Noordhoff, Groningen, 1970.

[29] J.P. LaSalle, The Stability of Dynamical Systems, Society for Industrial and Applied Mathematics, 1976. https://doi.org/10.1137/1.9781611970432.

[30] A.M. Lyapunov, The General Problem of the Stability of Motion, Int. J. Control 55 (1992), 531–534. https://doi.org/10.1080/00207179208934253.

[31] M.-J. Wang, F. Chen, J.T.Y. Lau, Y.-P. Hu, Hepatocyte Polyploidization and Its Association with Pathophysiological Processes, Cell Death Dis. 8 (2017), e2805. https://doi.org/10.1038/cddis.2017.167.

[32] H. Dahari, A. Lo, R.M. Ribeiro, A.S. Perelson, Modeling Hepatitis C Virus Dynamics: Liver Regeneration and Critical Drug Efficacy, J. Theor. Biol. 247 (2007), 371–381. https://doi.org/10.1016/j.jtbi.2007.03.006.

[33] S.A. Gourley, Y. Kuang, J.D. Nagy, Dynamics of a Delay Differential Equation Model of Hepatitis B Virus Infection, J. Biol. Dyn. 2 (2008), 140–153. https://doi.org/10.1080/17513750701769873.

[34] J.M. Murray, S.F. Wieland, R.H. Purcell, F.V. Chisari, Dynamics of Hepatitis B Virus Clearance in Chimpanzees, Proc. Natl. Acad. Sci. U.S.A. 102 (2005), 17780–17785. https://doi.org/10.1073/pnas.0508913102.

[35] M. Renardy, C. Hult, S. Evans, J.J. Linderman, D.E. Kirschner, Global Sensitivity Analysis of Biological Multiscale Models, Curr. Opin. Biomed. Eng. 11 (2019), 109–116. https://doi.org/10.1016/j.cobme.2019.09.012.

[36] Z. Zi, Sensitivity Analysis Approaches Applied to Systems Biology Models, IET Syst. Biol. 5 (2011), 336–346. https://doi.org/10.1049/iet-syb.2011.0015.

[37] S. Marino, I.B. Hogue, C.J. Ray, D.E. Kirschner, A Methodology for Performing Global Uncertainty and Sensitivity Analysis in Systems Biology, J. Theor. Biol. 254 (2008), 178–196. https://doi.org/10.1016/j.jtbi.2008.04.011.

[38] A. Khan, R. Zarin, G. Hussain, N.A. Ahmad, M.H. Mohd, A. Yusuf, Stability Analysis and Optimal Control of COVID-19 with Convex Incidence Rate in Khyber Pakhtunkhawa (Pakistan), Results Phys. 20 (2021), 103703. https://doi.org/10.1016/j.rinp.2020.103703.

[39] A.M. Elaiw, A.S. Alhmadi, A.D. Hobiny, Dynamics and Stability of a Within-Host HIV-HBV Co-Infection Model with Time Delays, Front. Appl. Math. Stat. 11 (2025), 1633039. https://doi.org/10.3389/fams.2025.1633039.

[40] S.R. Lewin, R.M. Ribeiro, T. Walters, G.K. Lau, S. Bowden, S. Locarnini, A.S. Perelson, Analysis of Hepatitis B Viral Load Decline Under Potent Therapy: Complex Decay Profiles Observed, Hepatology 34 (2001), 1012–1020. https://doi.org/10.1053/jhep.2001.28509.